

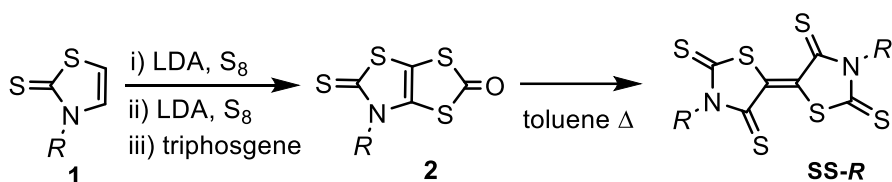
## Supporting Information

### Temperature-dependent characteristics of n-channel transistors based on 5,5'-bithiazolidinylidene-2,4,2',4'-tetrathiones

Suho Ryo,<sup>a</sup> Dongho Yoo,<sup>a</sup> Kodai Iijima,<sup>a</sup> Ryonosuke Sato,<sup>a</sup> Yann Le Gal,<sup>b</sup> Dominique Lorcy,<sup>b</sup> and Takehiko Mori<sup>\*a</sup>

#### Synthesis

All commercial chemicals and solvents were used without further purification. Amylamine (A0445), and hexylamine (H0134) were obtained from TCI. Carbon disulfide (038-01246) was obtained from Wako. The data of Nuclear Magnetic Resonance spectrum (NMR) and Mass spectrum (MS) were obtained with a JEOL JNM-AL300 spectrometer and a JEOL JMS-Q1050GC mass spectrometer, respectively.



#### 3,3'-Dimethyl-5,5'-bithiazolidinylidene-2,4,2',4'-tetrathione (SS-R).

Under nitrogen atmosphere, to a  $-10\text{ }^{\circ}\text{C}$  cooled solution of *N*-alkyl-1,3-thiazole-2-thione **1** (7.6 mmol)<sup>8</sup> in dry THF (50 ml) was added a solution of lithium diisopropylamide (LDA) freshly prepared from *n*-butyl lithium (*n*-BuLi) (11.5 mmol, 7.2 mL) and diisopropylamine (11.5 mmol, 1.6 mL) in 30 mL dry THF. After stirring for 30 min at  $-10\text{ }^{\circ}\text{C}$ , S<sub>8</sub> (11.5 mmol, 366 mg) was added and the solution was stirred for additional 30 min. To the medium, a solution of LDA freshly prepared from *n*-BuLi (15.3 mmol, 9.6 mL) and diisopropylamine (15.3 mmol, 2.2 mL) in 30 mL dry

THF was added. The reaction mixture was stirred at  $-10\text{ }^{\circ}\text{C}$  for 3 h and sulfur  $\text{S}_8$  (12.6 mmol, 403 mg) was added. After 30 min, triphosgene (11.4 mmol, 3.38 g) was added and stirred for 30 min at  $-10\text{ }^{\circ}\text{C}$  and further stirred at room temperature overnight. The solution was evaporated *in vacuo* and extracted with dichloromethane and washed with water. The organic layer was dried over  $\text{MgSO}_4$  and evaporated *in vacuo*. The crude product was purified by column chromatography using dichloromethane as eluent to afford **2** as a brown solid.

A solution of **2** in 50 mL toluene was refluxed overnight. 90% of the solution was evaporated *in vacuo* and the precipitate was filtered and washed with ethanol and dried *in vacuo* to afford **SS-R** as a black solid. Crystals of sufficient quality for X-ray diffraction were obtained by slow evaporation of  $\text{CH}_2\text{Cl}_2$ .

**SS-Pen**: Yield: 45% (740 mg).  $^1\text{H}$  NMR (300MHz,  $\text{CDCl}_3$ )  $\delta$  0.98 (t, 3H,  $\text{CH}_3$ ,  $J = 7.4$  Hz), 1.74 (m, 2H,  $\text{CH}_2$ ), 1.38 (m, 2H,  $\text{CH}_2$ ), 3.78 (m, 2H,  $\text{CH}_2$ ); HRMS (ASAP) calcd for  $\text{C}_{16}\text{H}_{22}\text{N}_2\text{S}_6$   $[\text{M} + \text{H}]^+$ : 434.776. Found: 434.8932; Anal. calcd for  $\text{C}_{16}\text{H}_{22}\text{N}_2\text{S}_6$ : C, 44.20; H, 5.10; N, 6.44. Found: C, 43.96 ; H, 4.87; N, 6.18.

**SS-Hex**: Yield 48% (840 mg).  $^1\text{H}$  NMR (300MHz,  $\text{CDCl}_3$ )  $\delta$  0.98 (t, 3H,  $\text{CH}_3$ ,  $J = 7.4$  Hz), 1.78 (m, 2H,  $\text{CH}_2$ ), 1.35 (m, 2H,  $\text{CH}_2$ ), 3.88 (m, 2H,  $\text{CH}_2$ ); HRMS (ESI) calcd for  $\text{C}_{12}\text{H}_{14}\text{N}_2\text{S}_6$   $[\text{M} + \text{H}]^+$ : 462.828. Found: 462.9562; Anal. calcd for  $\text{C}_{12}\text{H}_{14}\text{N}_2\text{S}_6$ : C, 46.72; H, 5.66; N, 6.05. Found: C, 46.62; H, 5.46; N, 6.14.

### **Cyclic Voltammetry (CV) and ultraviolet-visible spectroscopy (UV-Vis)**

Redox potentials were measured by cyclic voltammetry. Dry dichloromethane was used as a solvent,  $\text{Bu}_4\text{N}\cdot\text{PF}_6$  as an electrolyte and ALS-701E as a measuring instrument. An  $\text{Ag}/\text{AgNO}_3$  electrode was used for the reference electrode, and glassy carbon and platinum electrodes were used for the working electrode and the auxiliary electrode, respectively.

Ultraviolet-visible absorption spectra were measured at room temperature using a quartz cuvette having a 1 cm path using a UV-1800 ultraviolet-visible spectrophotometer (Shimadzu). Dichloromethane was used as a solvent. With increasing the alkyl chain length, the splitting of the 500-600 nm peak became less important probably because it is related to the intermolecular interaction. The optical band gap (HOMO-LUMO gap) was calculated from the edge of the visible absorption band.

## Crystal Structures

The X-ray oscillation photographs for **SS-Pen** were taken using a RIGAKU R-AXIS RAPID II imaging plate with  $\text{CuK}\alpha$  radiation from a rotation anode source with a confocal multilayer X-ray mirror (RIGAKU VM-Spider,  $\lambda = 1.54187 \text{ \AA}$ ). Diffraction data for **SS-Hex** were collected on a Rigaku AFC-7R four-circle diffractometer using  $\text{MoK}\alpha$  radiation from a rotation anode source ( $\lambda = 0.71069 \text{ \AA}$ ). The structures were solved by the direct method (SHELXT) and refined by the full-matrix least-squares method by applying anisotropic temperature factors for all non-hydrogen atoms using the SHELXL programs.<sup>S1,S2</sup> The hydrogen atoms were placed at geometrically calculated positions. Transfer integrals were estimated from the overlap of the molecular orbitals.<sup>26</sup>

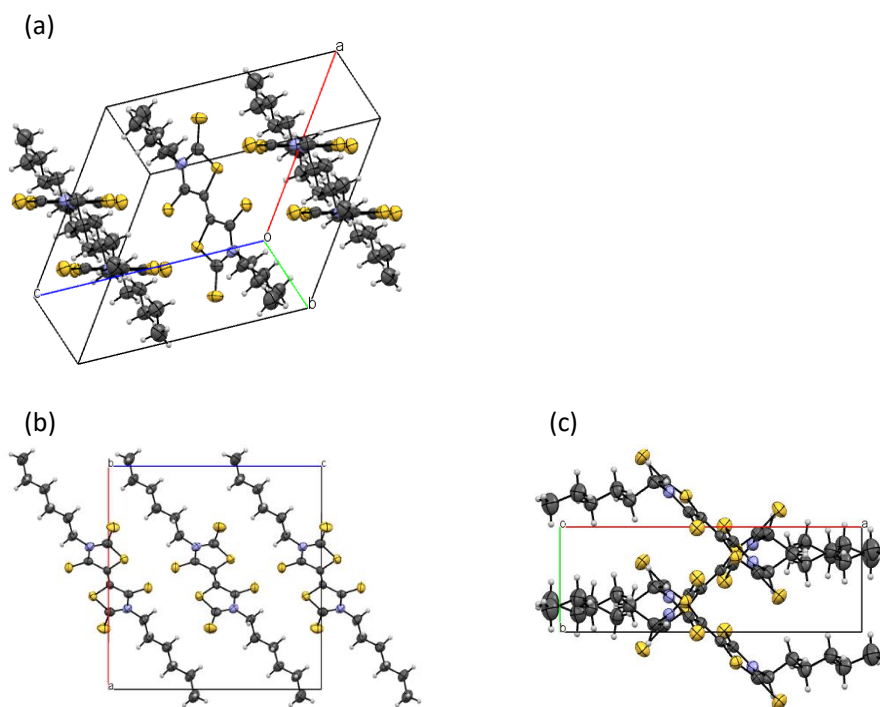


**Figure S1.** (a) Crystal structure of **SS-Hex** viewed along the molecular long axis. (b) Crystal structure of **SS-Hex** viewed along the *b* axis, and (b) along the *c* axis.

### **Thin film properties**

X-ray diffraction analyses of thin films (50 nm) on TTC (20 nm) were performed by X'pert-Pro-MRD using the  $\theta$ - $2\theta$  technique with Cu- $K\alpha$  radiation for  $2^\circ \leq 2\theta \leq 20^\circ$ . AFM images of thin films (50 nm) on TTC (20 nm) were taken by a SII scanning probe microscope system SPI3800N and SPA-300 by using a Si<sub>3</sub>N<sub>4</sub> cantilever.

## Transistor characteristics

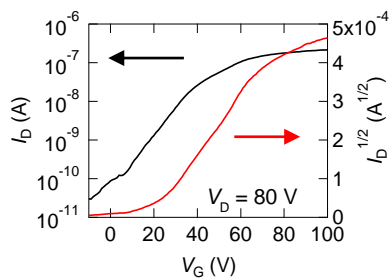


**Figure S2.** Transfer characteristics of an **SS-Hex** single-crystal transistor.

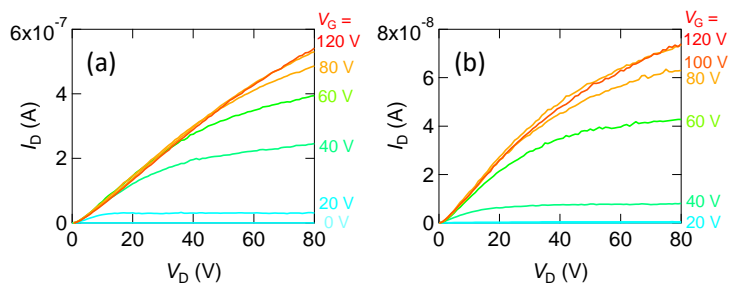


**Figure S3.** Output characteristics of single-crystal transistors measured at room temperature for (a) **SS-Pen** ( $I/b$ ), and (b) **SS-Hex** ( $I/b$ ).

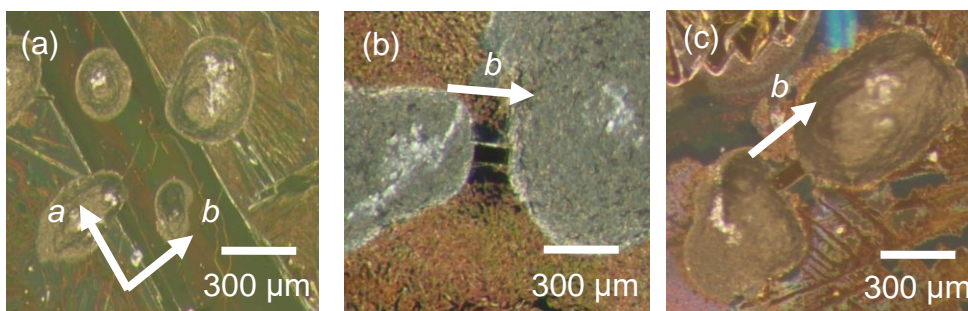


**Figure S4.** Single-crystal transistors of (a) **SS-Pr**, (b) **SS-Pen**, and (c) **SS-Hex**.

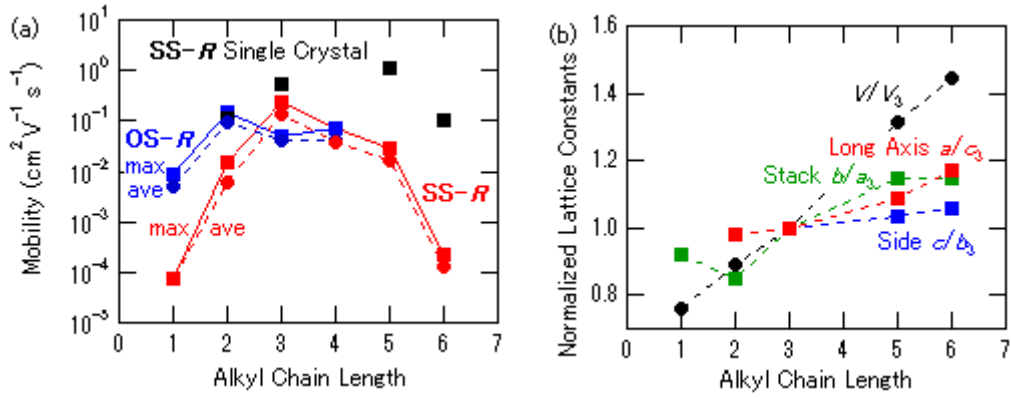


**Figure S5.** (a) Summary of mobility. (b) Lattice constants normalized by  $a_3 \sim c_3$  and  $V_3$  of SS-Pr.

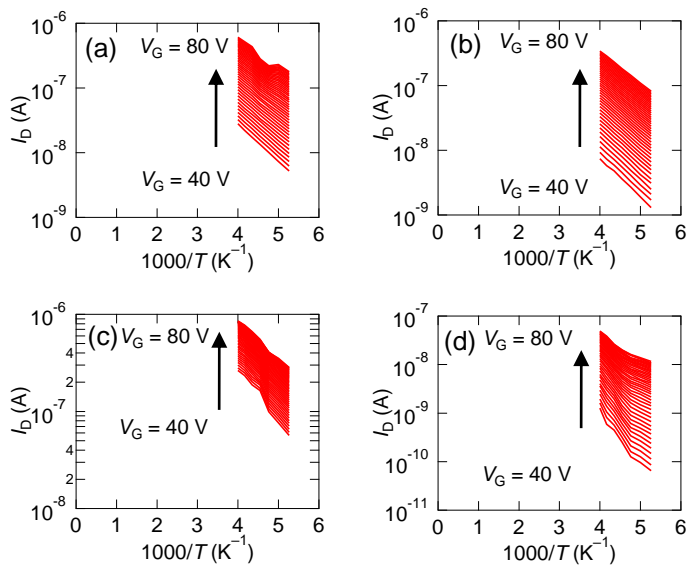


**Figure S6.** Arrhenius plots of  $I_D$  for transistors of (a) SS-Pr ( $//a$ ), (b) SS-Pr ( $//b$ ), (c) SS-Pen ( $//b$ ), and (d) SS-Hex ( $//b$ ).

## References

- S1 Sheldrick, G. M. SHELXT – Integrated Space-Group and Crystal Structure Determination. *Acta Crystallogr. A*. 2015, **71**, 3.
- S2 Sheldrick, G. M. Crystal Structure Refinement with SHELXL. *Acta Crystallogr. C*. 2015, **71**, 3.